Proceedings World Geothermal Congress 2023
Beijing, China, April 17 – 21, 2023

Calibration of a high enthalpy geothermal reservoir model utilizing micro-seismicity data

Dimitrios Karvounis[1], Raymi C. Castilla, Peter Meier, Sigríður Kristjánsdóttir, Vanille Ritz, Antonio P. Rinaldi, Vala HJÖRLEIFSDÓTTIR, and the COSEISMIQ Team

[1]Reitergasse 11, 8004, Zurich, Switzerland

d.karvounis@geo-energie.ch

Keywords: Hellisheidi, Husmuli, Geothermal Reservoir, Reservoir Simulation, Induced Seismicity

ABSTRACT

Large fractures play a crucial role in the performance and sustainability of geothermal power plants. They make certain regions more preferential for drilling new wells, they host many of the important flow paths in the reservoir that can disrupt power generation, and when large fractures in the reservoir are undetected then risks are high (e.g., financial, seismic, and contamination risks). Diffusion-induced micro-seismicity sheds light on many of these fractures away from the well. The risk of mismanaging these fractures can then be alleviated with a calibrated Discrete Fracture Model (DFM). Calibrating DFMs requires new workflows due to their novelty. The effort is justified because continuum models have limited validity to scenario testing and under-utilize the expensive to collect micro-seismic data.

Here, we present our workflow for calibrating an embedded DFM utilizing micro-seismicity data. The workflow uses the embedded DFM of the HFR-Sim simulator, which is the in-house simulator of ETH Zurich for Enhanced Geothermal Systems. The embedded DFM of HFR-Sim is specially designed for dynamically changing fracture networks and probabilistic predictions for diffusion-induced earthquakes. Necessary inputs to the workflow are the detected micro-seismicity data and the corresponding hydraulic logs. A likely representation of the ruptured fracture network is derived through a combination of physics-based modeling and unsupervised machine learning. The size of these fractures and their orientations are the ones that best explain the shape of the micro-seismic cloud and its migration. The fractures derived from the micro-seismic analysis, the deterministic fractures at the wells, and the continuum part of the embedded DFM are calibrated iteratively with successive HFR-Sim simulations, which simulations can take into account a plethora of typical field measurements.

We apply the workflow to the Husmuli (Húsmúli) zone in South West Iceland, where wastewater is injected since September 2011, a lot of micro-seismicity has been recorded, and for which several field measurements and tests exist. The zone is part of the high-enthalpy geothermal field Hellisheidi (Hellisheiði) with a power plant that produces 300 Mwe and 130 MWth. Calibrated fractures are extracted with the workflow, and are considered by the high-fidelity model of Husmuli. The model is then calibrated and reproduces the total injectivity of the five wells at the end of the considered period and the overall rate of seismicity.

1. INTRODUCTION

Reliably managing the large fractures of a geothermal reservoir is important for maximizing production, and revenue, and ensuring the sustainable operation of the power plant. Many expensive geothermal wells have been abandoned due to low injectivity or low productivity. This would not have been the case if large permeable fractures penetrated these wells. Fractures also host important flow paths that dominate the thermal breakthrough and the life expectancy of the power plant. Wells may have to be abandoned earlier than expected exactly because they are too well connected with these important flow paths. High-temperature geofluids can also migrate upwards due to sub-vertical large structures and then, geothermal wells near them can benefit by producing higher enthalpy fluids than expected.

Financial, seismic, and contamination risks can be high when fractures slip under the radar. Overall energy production will reduce with the thermal breakthrough from the reinjection of wastewater. The moment of this breakthrough can be too early because of fractures. Production can also decline if too many wells produce from the same permeable structures and reduce the pressure of the structure. Geothermal power plants need both wells for production and wells for reinjecting the cold geofluids. It is the relative positioning of the fractures that hints at the best locations to drill each type of well. Finally, one needs not neglect the seismic risk that can lead to undesired seismicity, as well as the risk of contamination. For example, pressure depleted reservoir may exhibit increased gasification. Fractures can be undesired conduits for this gas to reach the surface.

Explicit modeling of large fractures with a Discrete Fracture Model (DFM) is more accurate than employing equivalent porous media (Zareidarmiyan et al., 2021, Moinfar et al., 2012). But the scarcity of information on the fractures away from the wells is a hindrance to employing DFMs since it is not straightforward how to calibrate them. Analysis of images from the wells and from outcrops provide some information for the statistical properties of the fracture network at these locations. Out of this information and with an approximation for the in-situ stress conditions, one can stochastically generate Discrete Fracture Networks (DFN) that satisfy the observations and have similar effective properties. An example of such a workflow is the DFN designed for the FORGE site in Utah (Golder Associates Inc.., 2020).

Both passive and active seismic monitoring are sources of valuable information for the structures away from the wells. An extended network of seismometers that are sensitive enough to detect seismicity can accurately locate points in the reservoir that should belong to fractures. Focal planes can also be extracted by processing the signal from all the seismometers, which focal planes return a pair of possible orientations for the fracture of the seismic event. The sensitivity of the monitoring systems has significantly improved

during the last decades. This has significantly increased the amount of information from injections since detected seismicity can be at the scale of micro-seismicity.

Here, a workflow is presented that utilizes the injection-induced micro-seismicity and calibrates a geothermal reservoir. The workflow returns a hydraulically calibrated DFM that reproduces the hydraulic logs and the catalog of seismicity. The workflow aims to supplement existing workflows for calibrating fractured reservoirs and is here implemented on real data collected from Husmuli, which is part of a high enthalpy geothermal reservoir in Iceland.

The Hellisheidi (Hellisheiði) geothermal field in South West Iceland (Figure 1) hosts one of the largest geothermal power stations in the world. It can generate more than *300* MW_e of electricity, and it also provides *130* MW_{th} of thermal power to the district heating of Reykjavik through a *20 km* pipeline (Gunnarsson et al. 2011, DiPippo 2016). The Hellisheidi power plant is an important asset for the decarbonization of Iceland and the carbon intensity of the plant ranks among the lowest of the geothermal technologies (Paulillo et al., 2019). Also, the injection of CO_2 and H_2S emissions take place, as part of the CarbFix project (Ratouis et al., 2019). A significant portion of the plant's annual emissions are permanently stored in basaltic subsurface rocks (Sigfusson et al, 2018). The field is located on the active volcanic system of Hengill, which hosts more than *70* geothermal wells (Sveinbjornsson and Thorhallsson, 2013) and more than 30 of these wells produce hot water for Hellisheidi.

Reinjecting the wastewater is necessary for maintaining high pressure in Hellisheidi because the production density is too intense for the designed power plant (Gunnarsson and Mortensen, 2016). Approximately *0.5* m^3/s of brine needs to be managed after leaving the power plant at a temperature of *120*^{o} *C* during warm months and of *90*^{o} *C* during the cold months when the district heating operates (Gunnarson 2013). Currently, there are two zones for reinjection, the Grahnukar (Gráhnúkar) and the Husmuli (Húsmúli) zones. The reinjection zone in Grahnukar was developed first. The formation there is found to be of high temperature (above *300*^{o} *C*), and the development of another zone for reinjection was decided. Producing from Grahnukar would be preferable to injecting cold wastewater. The new zone was developed in Husmuli, which proved to be colder than Grahnukar, but the wells in Husmuli did not achieve the total injectivity required for stopping injections in Grahnukar (Gunnarson, 2011). The initial total injection rate of *0.6* m^3/s in Husmuli dropped to *0.4* m^3/s.

Flow rates in Husmuli have been kept low by the operators because of important induced seismicity that started with the injection there. The largest seismic event reached magnitude M4 (Gunnarson 2013). Induced seismicity with magnitudes up to M2.3 was already observed during the drilling of wells in Husmuli, indicating the existence of critically stressed fractures (Gunnarsson 2013). Most of the deformation occurred during the first months after the start of the injection (Figure 3) indicating that an increase in pore pressure is a very plausible mechanism for the observed seismicity (Juncu et al., 2020). The focal mechanisms of the earthquakes had a right-lateral strike-slip with small components of normal faulting, which indicates that the direction of the least principal stress is near horizontal.

Initially, a one-flow model was considered for Hellisheidi, which one-flow is a conceptual model with one deep source of heat inside a very permeable single medium. Continuum Fracture Models (CFM) have been employed both for Hellisheidi and for Husmuli since the conceptual model is of low complexity and a CFM can be easily implemented. But the structure of the reservoir has proven to be more complicated than that. Fractures seem to form an extended complex network. Formation temperature has important narrow anisotropies and is discontinuous, indicating the existence of important fractures and shallower sources of heat (Gunnarsson and Mortensen, 2016). Tracers injected are soon recovered by nearby wells, indicating a very permeable but narrow hydraulic connectivity between the wells (Ratouis et al., 2019). CFMs calibrated on the tracer tests predicted a significant drop in the produced enthalpy, which prediction did not proven correct yet (Mahzari et al., 2021). The failure to predict the produced enthalpy highlights the need for a more complex conceptual model than the one-flow model.

A fractured model started being compiled by the operators that include all observations from Hellisheidi and is based on the software Leapfrog (Poux et al., 2018). The new structural model considers a few tens of vertical fractures that have limited interconnectivity, their orientations are based on observations from the surface and from televiewer data from the wells (Figure 1). The structural model does not extend below the wells, although this is where most of the injection-induced seismicity occurred. Here, we aim to supplement this effort by characterizing the fractures below the wells based on their seismic behavior.

We construct a structural model of Husmuli for the seismically active part of the reservoir and we calibrate the hydraulic parameters of a DFM. The DFM is the one employed by HFR-Sim, which is the in-house simulator of ETH Zurich for Enhanced Geothermal Systems (EGS), and it employs an embedded DFM especially designed for dynamically changing fracture networks. HFR-Sim can model the Thermal-Hydraulic-Mechanical-Seismic processes inside an EGS reservoir (Karvounis and Jenny 2016, Deb and Jenny, 2017a, 2017b, 2017c) and an optimized version exists that considers only modeling of flow and of seismicity (Karvounis and Wiemer, 2022). Here, the latter accelerated version is considered; i.e., flow is the only process modeled and there is minimal thermal and seismic modeling. An important advantage of HFR-Sim is its high versatility that allows dynamically increasing the number of fractures inside a reservoir for maximum structural fidelity.

First, we present the workflow and then two of its main elements for calibrating the structural model: i.e., the DFM of HFR-Sim and the unsupervised Machine Learning approach required for extracting alignments. Then the workflow is implemented into real data from Husmuli that have been kindly provided to us by ISÓR, Reykjavík Energy, and the Icelandic Meteorological Office (IMO) for the needs of the COSEISMIQ project (www.coseismiq.ethz.ch/en/home/).

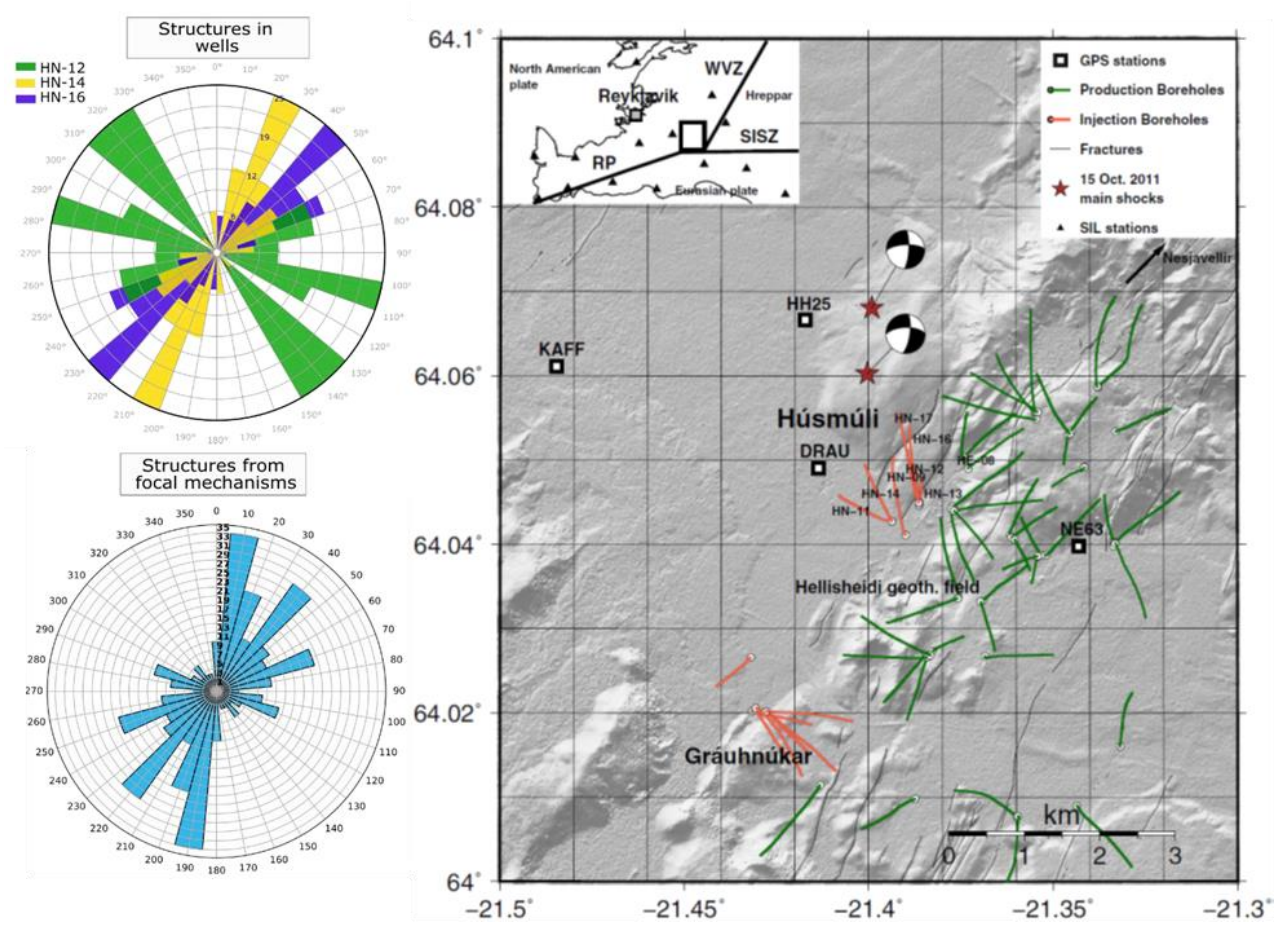

Figure 1 On the left, the orientation of structures observed from well-images and from the focal mechanisms in Husmuli. On the right, a map of Hellisheidi that is adapted by Juncu et al., 2020, and shows the high density of boreholes in the area.

2. WORKFLOW

A workflow is described here for high enthalpy geothermal reservoirs that exhibit unexpected seismicity from reinjecting cold wastewater and their structural model needs to be revisited. The main aim of the workflow is to find the Discrete Fracture Network (DFN) that spatiotemporally reproduces the observed injection-induced seismicity. The final product of the workflow is a structural model that reproduces both the hydraulic logs and the seismicity due to reinjection.

The workflow is based on iteratively simulating structural models with the HFR-Sim simulator. HFR-Sim is the in-house simulator of ETH Zurich for Enhanced Geothermal Systems (Karvounis 2013) that can perform thermo-hydro-mechanical modeling. It employs an adaptive Hierarchical Fracture Representation (aHFR) modeling approach specially designed for dynamically changing fracture networks (Karvounis and Jenny 2015). A hybrid version of HFR-Sim has been created and optimized for probabilistic predictions of diffusion-induced seismicity (Karvounis and Wiemer, 2021) that aims to assist in real-time prediction and control of the seismic risk in EGS, as well as in safely maximizing production in geothermal systems with seismicity.

Initially, a continuum domain called matrix is considered that is going to be the basis of our structural model and it is going to be part of the HFR-Sim model. This continuum domain integrates all field observations that are well comprehended and reliable, but they are not characterized in detail. Examples of such observations are the inter-well transmissibility and the geothermal gradient. The effective value of the former can be found with simple injection tests. Continuum Fracture Models (CFMs) (Barenblatt et al., 1960) are significantly simpler than DFMs and can match such sparse observations with little effort. Embedded DFMs, such as the aHFR approach combines the advantages of both the DFM and CFM. They can utilize both calibrated CFMs (e.g. the permeability field of a TOUGH-2 model) and the plethora of structural field observations that require models with high fidelity for the thin fractures that penetrate the well.

Such structural observations are treated by HFR-Sim with deterministic domains that are embedded into the basis-continuum. The main deterministic elements are the trajectories of the wells and all the fractures with significant mud losses during their drilling. Excessive mud losses indicate structures with important injectivity. The orientation of these fractures is also deterministic when well-bore images exist. It is the shape and the hydraulic properties of these deterministic fractures that are unknown and need to be assessed in conjunction with the matrix's effective properties. This task is not our focus here, since such simple DFMs scenarios are easy to calibrate with any DFM. But such a calibrated DFM is considered the starting point of our workflow.

In addition to the above deterministic fractures, also less deterministic fractures are added. The characteristics of these fractures are our focus here. We focus on two families of fractures: (i) pre-existing fractures called ‘alignments’ that steer diffusion processes and (ii) seismic fractures. Alignment fractures are the result of post-processing the catalog of micro-seismicity. They are manifolds of

minimal complexity with directions that follow the propagation of seismicity. Seismic fractures are disk-shaped fractures centered around each micro-seismic location, representing the ruptured surface of the event. Their orientation is not known with certainty, but educated guesses are possible when the stress conditions are known. Even better, when a focal plane solution exists. Seismic fractures are discretely represented in our DFM only after they have been triggered. These seismic fractures are very similar to the random seed fractures of the hybrid DFM (Karvounis and Wiemer, 2022). As the case is for the hybrid DFM, a failure over-pressure Pf is assumed. This Pf should be as close to the possible expected overpressure for hydro-shearing to occur. The relative positioning of the seismic fractures is as good as the relative positioning of the seismic catalog. Alignment fractures alleviate the risk of a catalog with large absolute errors.

The HFR-Sim model of the workflow consists of the matrix, the wells, the deterministic fractures, the alignments, and the seismic fractures. It also includes their hydraulic properties (mainly permeability, viscosity, and diffusivities) and a Pf distribution for seismic fractures. Initially, the number of alignment fractures is corrected in order to avoid overfitting. This step is done by assigning high diffusivity to all the non-deterministic fractures and then correcting if large volumes of the reservoir are over-pressurized and no seismicity is detected there. Within a few iterations, one could find the best-fitting subset of the alignment fractures. This first step is the calibration of the structural model.

The next step is calibrating diffusivities. Here, this includes two subtasks that are not strongly dependent and can be calibrated against different sets of data. The permeability of the deterministic fractures and the diffusivity of the matrix must best fit the final injectivity of the wells. The diffusivity of the fractures must best fit the observed seismicity; i.e., the time moments at which pressure Pf is exceeded must have a similar rate to the observed seismicity. These two steps are not strongly dependent, because injectivity tends to be dominated by the nearby structures, while seismicity occurs on structures that are also away from the wells. The workflow is schematically sketched below in Figure 2.

The final result of the workflow is a DFN with calibrated transmissivities. The transmissivity of a fracture is defined as

$$T = \frac{b^3}{12\mu}\rho g, \tag{1}$$

where b is the hydraulic aperture of the fracture, μ the viscosity, ρ the density, and g is the acceleration of gravity. Freshwater conditions are considered for all transmissivities reported here.

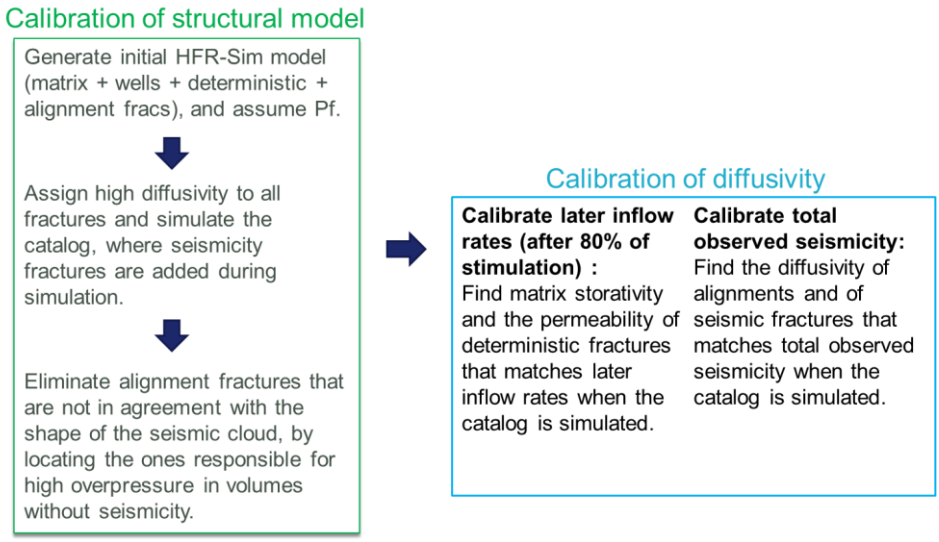

Figure 2 The Algorithmic Framework of the Calibration's Workflow.

3. HFR-SIM: DISCRETE FRACTURE MODEL

Here, the optimized version of HFR-Sim is employed for fast simulations of single-phase linear pressure diffusion (Karvounis and Wiemer, 2012). Neither stress changes nor heat transport nor stochastic seismicity are considered. Pore pressure diffusion initiates from the injectors, it then propagates inside the Discrete Fracture Network (DFN) and inside the surrounding matrix. The DFN considered by HFR-Sim is not steady but it changes with important seismicity and according to the located seismicity. The domain of the i-th discrete fracture is denoted as Ω_i and is modeled as a two-dimensional manifold embedded in a three-dimensional domain Ω that has effective properties for the rest of the structures inside a geothermal reservoir.

The main partial differential equation solved is the single-phase mass conservation equation that at time moment t is expressed inside the reservoir's three-dimensional domain Ω (matrix) as

$$S\frac{\partial p}{\partial t} = \nabla \cdot \left(\frac{\boldsymbol{k}}{\mu} \cdot \nabla p\right) + q + Q + \Sigma q_i^f, \tag{2}$$

where S, p, $\boldsymbol{k}$, μ, q, Q are compressibility, pressure, the tensor of permeability that is anisotropic along fractures, fluid viscosity, the reinjection rate from the well, and the rest of the natural sink/source terms (e.g., far field boundaries). The source term q^f accounts

for the mass exchange between the reservoir and important fractures embedded into it that are treated discretely as two-dimensional manifolds and HFR-Sim solves mass conservation inside it

$$S^f \frac{\partial p^f}{\partial t} = \nabla \cdot \left(\frac{b_i^2}{12\mu} \cdot \nabla p^f \right) + q - q_i^f , \quad (3)$$

where b_i is the hydraulic aperture of the i-th discrete fracture and the cubic law has been considered for the permeability of the fractures. Here, and without loss of generality, thermal effects like gravity-driven flow ('buoyancy') or non-linear phenomena (e.g. fracture dilation) are not considered. One should carefully balance the necessity for more governing equations with the risks of overfitting/underfitting. Here, we consider a rather simple scenario where only pressure diffusion is numerically solved.

Both the deterministic and the alignment fractures are highly permeable throughout the simulations with HFR-Sim. The seismic fractures become permeable at the time moment they fail. The Mohr-Coulomb failure criterion is used for estimating a proxy of the failure pressure P_f of every seismic fracture Ω_i. The time moment of their shearing is numerically estimated by finding the time-moment where $p>P_f$. According to the criterion, an induced seismicity event with hypocenter X_s and source time t_s occurs only if the pressure there equals to

$$p(X_s, t_s) = P_f = \frac{C_0 - \tau}{\mu_s} + \sigma_n , \quad (4)$$

where σ_n and τ are the normal compressive stress and the shear stress on the seismic fracture, C_0 is cohesion and μ_s the friction of a fault.

The governing equations solved are like the ones of the Discrete Fracture Hybrid Model (Karvounis and Wiemer, 2022). An important difference from the model presented there is the shape of the seismic fractures. There, all fractures are two-dimensional manifolds, while here this is the case only for the deterministic and the alignment fractures. Seismic fractures consist of two two-dimensional disks crossing each other at the center and with a fixed distance between their tips. This is an unrealistic shape for small fractures, but it improves interconnectivity of small fractures that are parallel and numerically is equivalent to having a single fracture with twice the conductivity.

4. UNSUPERVISED MACHINE LEARNING FOR EXTRACTING ALIGNMENT FRACTURES

Alignment fractures are a necessary assumption for building the structural model when the hypocenters of a catalog are associated with large errors and as a result, their distribution looks more like a cloud and less like a plane. The main reasoning behind their modeling is that seismicity migrates along them and not towards any direction. Given the absence of solid proofs for their existence, unsupervised Machine Learning algorithms are employed for clustering the found hypocenters and extracting their best-fitting planes.

Firstly, the observed seismic locations and origin times are clustered with a Bayesian Gaussian Mixture Model (BGMM). BGMM models the density of seismic events by combining a so-called 'Chinese Restaurant' process with the Expectation Maximization (EM) algorithm. The former is a stochastic process that can partition the training set and then EM can fit a Gaussian to every partition. The result of BGMM is a mixture of Gaussian Distributions that best fit the density of the training data, and each of the training data can be clustered with the fitted Gaussians. An advantage of BGMM is that one does not need to specify from the beginning the number of Gaussians required. BGMM returns both an optimal number of Clusters and their properties.

Once the seismic locations are clustered with BGMM, then a best-fitting plane is found for each cluster with Principal Components Analysis (PCA). PCA is again a standardized unsupervised ML algorithm that can reduce the dimensions of a point cloud into the best fitting plane. Here, PCA is performed only for the spatial features of the catalog and for clusters with at least 3 events. Note that this is not the case for the Clustering with BGMM, where we assume that the time component is also important. Candidate alignment fractures are rectangle-shaped and their lengths increase with the size of their respective cluster in each of its two principal directions.

As a final step for building the structural model, cross-validation is necessary. The clustering process described above is not immune to overfitting when it comes to predicting/inferring. The goal of the cross-validation is to eliminate any alignment fractures that over-fit the catalog. We do so, by assigning an unrealistic high diffusivity to all three families of fractures in the DFN (deterministic, seismic, and alignment fractures) and assuming a mean value for P_f. Then, equations (1) and (2) are numerically solved for the hydraulic logs. Alignment fractures that pressurize certain partitions of the matrix with more than Pf can be easily identified. When seismicity has not been observed in these partitions, then their nearest alignment can be omitted from the set and the governing equation can be solved again. If the new number of over-pressurized partitions with observed seismicity remains like before, then this alignment can be omitted from the set of fractures.

5. IMPLEMENTING THE WORKFLOW FOR HUSMULI

Reinjection in Husmuli started in September 2011 from the deepest of the wells in the area called HN-09. Within the next weeks, waste-water started being reinjected into the rest of the wells with the following order HN-14, HN-12, HN-17 and finally HN-16. Seismicity started being detected with the reinjection in HN-12 and many bursts of seismicity were recorded during the following 9 months (Figure 3). Here we utilize the micro-seismicity collected during these first 9 months of reinjection in order to calibrate a structural model for Husmuli.

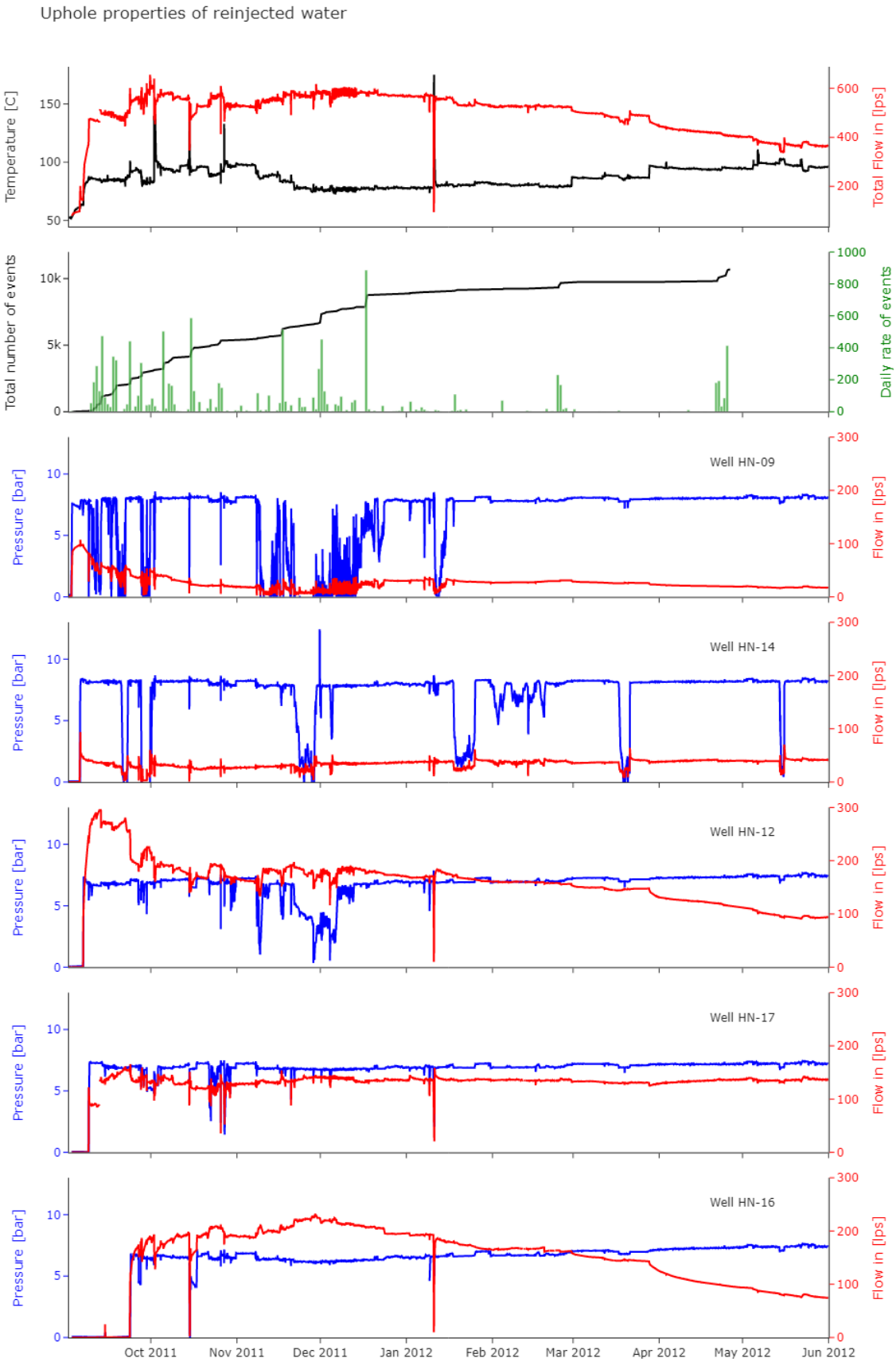

Figure 3 Hydraulic and temperature logs from the reinjection wells in Husmuli and the rate of seismic events associated with the reinjection. The wells are sorted with their starting times for waste-water reinjection.

5.1 Matrix, boundary conditions and deterministic fractures

For the matrix, a large-scale TOUGH2 model for the Hengill geothermal field was utilized which was provided by Reykjavik Energy. The model for Hengill covers an area of 50 km x 50 km and reaches a depth of 3000 m. In HFR-Sim a vertical cuboid is considered with dimensions 3.3 km × 7 km × 5.625 km, and rotated N40^0. For depths above 1.5 km the mean permeability of the TOUGH2 tensor is considered. This permeability reproduces past tracer tests from the area, but no seismicity. For depths below 1.5 km permeability is set to the low value of $10^{-17}\ m^2$. The rotation of the cuboid is performed to better align it with seismicity and to reduce its volume while it still includes the majority of the relocated seismicity (more than 95% of it). Dirichlet boundary conditions with fixed zero overpressure are considered for the top surface of the cuboid. For the other five sides of the cuboid, no-flux conditions are assumed. Dirichlet are the boundary conditions at the five wells. For simplicity, a less volatile pressure evolution is considered that also partially considers the strong correlation between the total inflow and the temperature that is seen in the hydraulic logs (Figure 3). More precisely, the median uphole pressure is estimated for each well and then we add to it the expected overpressure at its bottom when the well is filled with water of 90^{o}C. The values for the five wells are *2.3 MPa* for HN-09, *2.17 MPa* for HN-12, *2.21 MPa* for HN-14, *2.43 MPa* for HN-16, and *1.92 MPa* for HN-17. For the simulated scenario, uphole pressure for each well follows a step function and the step change in pressure happens at the moment reinjection starts in each well (Figure 3).

From the wells, only the five uncased segments are considered and their trajectories are reduced to straight lines. The drilling logs are utilized for locating highly permeable structures. A deterministic fracture is considered for every well location, where significant mud losses were observed. Aerial images have shown that the fractures at the outcrop consist of two large sets that are near vertical and orthogonal to each other (strike approx. 45^o and 135^o). When a wellbore image existed for a location with mud losses, then the orientation of the deterministic fracture was as in the image. When such an image does not exist, then two fractures are considered, centered at the spot with mud losses and their strike angles are as in the two sets from the outcrops. The deterministic fractures are squares of side *500m* and are shown in Figure 4. The size of the squares is arbitrarily chosen here. Typically, the size of such fractures can be found with analysis of the hydraulic logs, which step is not our focus here.

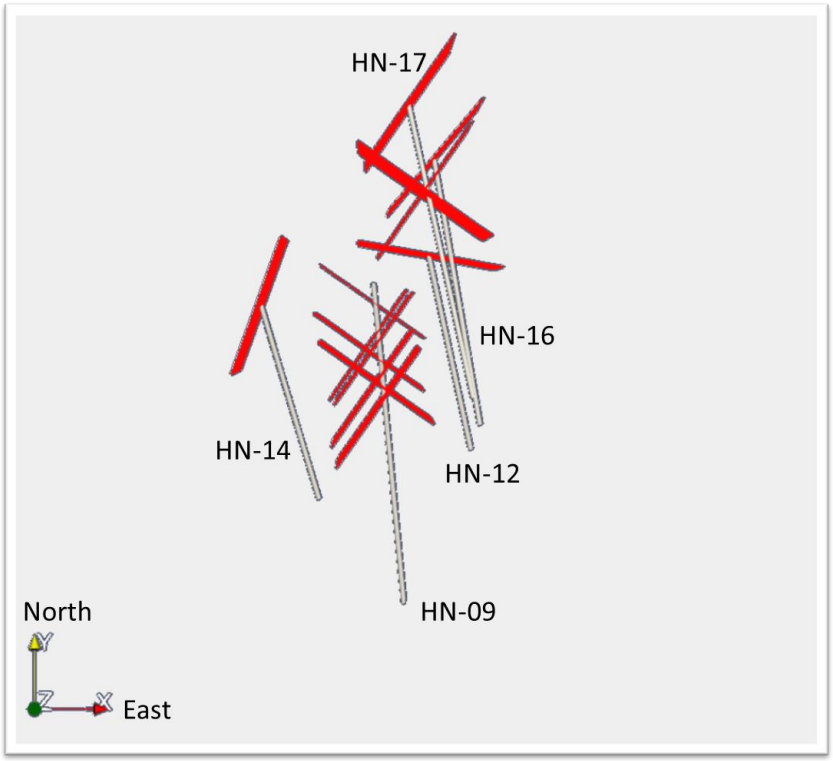

Figure 4 Mapview of deterministic fractures considered. They are centered at points of the wells with high mud losses. Their orientation is from televiewer images. When such an image did not exist, then outcrop information were utilized.

5.2 Stress model

For estimating failure pressure Pf, a stress model is required. Stress measurements in Husmuli are few (Batir et al., 2012) and the measured gradients do not confidently explain observed seismicity. The vertical stress Sv is the least uncertain stress and its value increases by 25 MPa per km of depth. Here, we consider the 369 focal mechanisms observed in Husmuli and a linear stress model is constructed that explains them. For every focal mechanism, the hydrostatic pressure is estimated by extrapolating the hydrostatic pressure of the deepest well HN-09 and Sv is estimated as in (Batir et al., 2012). Every focal mechanism consists of two planes that are auxiliary to each other. Here, we keep the plane that is most likely given the aerial and the wellbore images. Stochastic numerical experiments have shown that the focal mechanisms indicate an 'Andersonian' stress field; i.e. the vertical stress Sv is one of the three principal stresses (COSEISMIQ team, 2020). The three principal stresses are modeled as an Andersonian stress field with the linear functions

$$Sv = 25000 \cdot z$$
$$SH = SH_0 + SH_\zeta \cdot z, \text{ with trend } \varphi$$

$$Sh = Sh_0 + Sh_\zeta \cdot z, \text{vertical to } \varphi$$

where SH and Sh are the two principal horizontal stresses that are not necessarily SH>Sh, φ is the trend of one of them, SH_ζ and Sh_ζ are their gradients with depth z, and finally, SH_0 and Sh_0 are the intercept terms for the two linear models. An evolutionary optimization algorithm is employed for estimating the families of SH and Sh that best explain the observed focal planes. For every candidate combination of parameters $[SH_\zeta, Sh_\zeta, SH_0, Sh_0, \varphi]$, the shear and the normal stress are estimated on the plane. Then the number of planes is counted that cannot satisfy the Mohr-Coulomb criterion when cohesion is 0, friction within the range [0.6, 1] and Pf is positive and at most 3 MPa. The evolutionary algorithm converges after 73 iterations and its population includes 15 candidate solutions explaining the same maximal number of 311 out of 369 focal planes (approx. 85% success). The mean values and the standard deviation of these 15 optimal solutions are shown in Figure 5.
The inversion with the evolutionary algorithm shows that current data are too few. For many of the focal mechanisms one could conveniently assume an acceptable friction that returns a Pf in the acceptable range. For that reason, we assume *Pf=1 MPa* for all seismic events and all focal mechanisms. This homogeneous Pf model is the simplest that can be but it is not an overfit for the few stress observations.

Depth gradient of SH - SH_ζ	$(10684 \pm 14)\ Pa/m$
Depth gradient of Sh - Sh_ζ	$(11166 \pm 158)\ Pa/m$
Intercept term of SH-SH_0	$(3.675 \pm 0.035) \cdot 10^6$ Pa
Intercept term of Sh - Sh_0	$(2.8 \pm 0.301) \cdot 10^6$ Pa
Trend of SH – φ	138.2±3.5 degrees

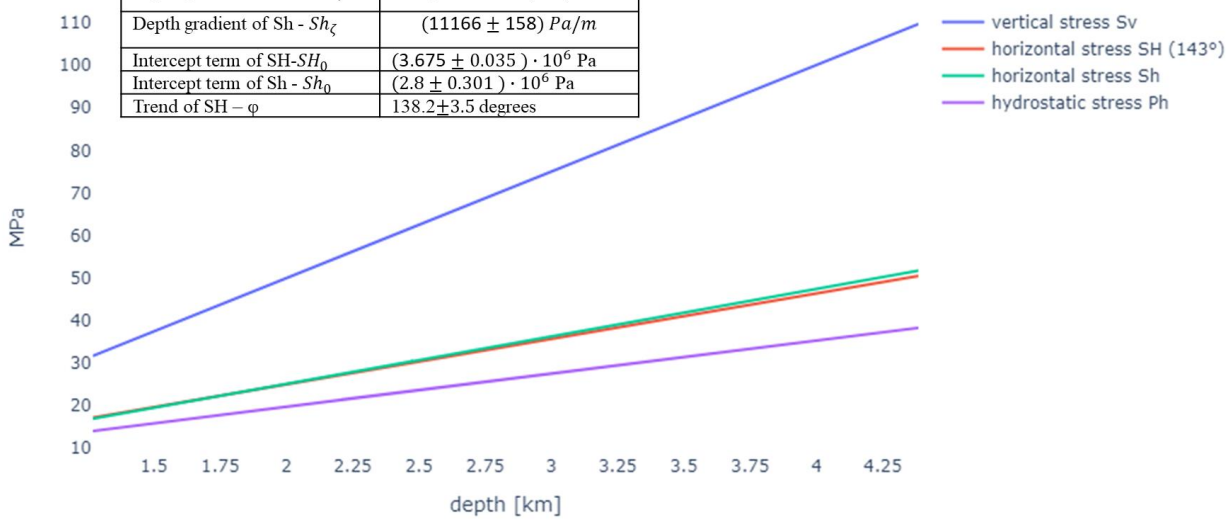

Figure 5: Initial stress field considered for the reservoir in Husmuli. In parenthesis in the table are the mean values and the standard deviation of the equally-probable optimal candidate solutions. One of these optimal stress models is plotted.

5.3 Catalog of seismicity and seismic fractures

Thousands of injection-induced seismic events have been recorded in Husmuli for the considered period (Li et al., 2019). These events have been relocated for the needs of Work Package 3 in COSEISMIQ (S. Kristjánsdóttir, 2018, COSEISMIQ team, 2020) and the relocated positions have served as the input seismic catalog for the workflow. The 10942 relocated positions of the catalog and their source times are shown in Figure 6.

This relocated catalog is an early version of the catalog compiled for COSEISMIQ and does not have magnitudes. Here, we fill this gap by matching the source times of these events with the source times of the official catalog from Husmuli obtained by the Icelandic Meteorological Office (IMO). This catalog has ML and ML2 values for the magnitude of the events. For each event from IMO, a moment magnitude Mw is estimated from ML and ML2 as described in Edwards and Douglas (2013). Then a nearest neighbor algorithm is employed that assigns to each relocated event the Mw of its nearest neighbor in time. The source times do not match perfectly. For 10.2% of the IMO events it is not clear which is their corresponding relocated event. The seismic catalog considered henceforth is the synthesis of the relocated position with a good match to the IMO catalog. The completion magnitude for Mw is found to be near 1.7.

For each event in the synthetic catalog with Mw ≥1.7, a strike and a dip are considered. The values of the two angles are estimated again with the nearest neighbor algorithm that returns the dip and the strike of the nearest in-space focal plane solution. The same set of 369 focal planes is considered here, which is also considered in section 5.2 Stress model, for which focal mechanisms the most likely of its auxiliary planes is considered given the televiewer and aerial images from Husmuli.

Henceforth, seismic fractures are treated like squared seeds; i.e., squared fractures that have low transmissivity until they exceed for the first time an overpressure of *Pf=1 MPa*. From that moment on, their transmissivity increases significantly. HFR-Sim considers a new fracture for each seed with Mw>2.1, which is a threshold value that depends on the grid-block size of the matrix cells. For each such seed with Mw>2.1, an equation like equation (3) needs to be solved. For seeds with Mw<2.1, it is the effective permeability of the matrix k that is updated in equation (2) and an additional equation does not need to be solved. As in the DFHM, the total number of fractures increases dynamically as more hypocenters exceed their respective Pf. Contrary to the DFHM, the shape of the added fractures is not a disk with the angles of the focal plane. Each seismic fracture consists of two two-dimensional squares forming an X-shape centered at the hypocenter. The X-shape is chosen in order to increase the number of seismic fractures that are interconnected. Fractures that are almost aligned and with the same orientation, have higher chances to intersect with each other.

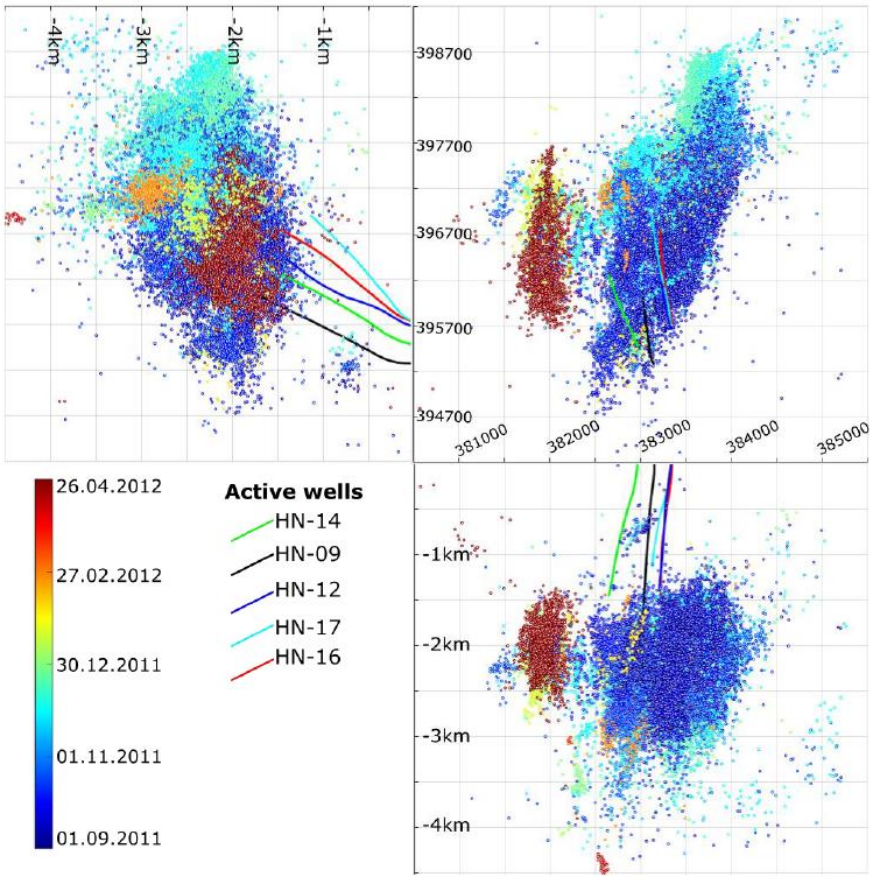

Figure 6 Map of the seismicity in the Husmuli area for the considered period (seismic catalog: S. Kristjánsdóttir, 2018). Figure adapted from COSEISMIQ (3rd Deliverable, 2020).

5.4 Alignment fractures

The Cartesian coordinates and source times of the relocated catalog of seismicity (Figure 6) are used for training the Bayessian Gaussian Mixture Model of section 4. The Dirichlet process returns that more than 95% of the relocated catalog can be modeled with approximately 43 Gaussians. The covariance matrix for each Gaussian is estimated, each relocated catalog is clustered to its most likely Gaussian and then a best-fitting plane is extracted for each Gaussian with the PCA. A total of 43 planes are obtained, out of which 42 pass the cross-validation test. The alignment fractures are squares of a side that is a multiple of the standard deviation of their respective Gaussians (6 times) or at least 1 km long.

For the cross-validation of the fractures, a set of seeds is created that consist of the seismic fractures and of a second set of seeds. The second set of seeds is benign and has no effect on a simulation with HFR-Sim. The locations of its seeds are equally spaced in the three-dimensional matrix, have also Pf=1, and no other properties are needed. Triggering a seed from this benign set is treated like a 'False-positive' because the simulation returns a seismic event that never happened. In contrast, triggering a seed from the seismic fractures is a 'True-positive' because the simulation returns a seismic event that happened in this location. During the cross-validation, the same catalog is simulated with a very high transmissivity for both the seismic and the alignment fractures. The subset of PCA planes is found that best balances between the desired 'True-positive' and the undesired 'False-negative' scenarios when HFR-Sim simulates this subset. Here, we had to omit only one PCA plane. The rest of the fractures are treated as alignments and aim to capture the main paths of seismic dispersion.

5.5 Results

The hydraulic parameters of the HFR-Sim model are calibrated to match the later inflow rates and the rate of seismicity in Husmuli. The calibration is performed semi-manually since a good match is proven possible with a few simulations. The simulated inflow and seismicity rate are plotted in Figure 7. The transmissivities that best match the observations are 4.2×10^{-4} m^2/s for the deterministic fractures, 1.1×10^{-4} m^2/s for the alignments, and $1.5 \cdot 10^{-4}$ m^2/s for the seismic fractures. The storativity of the fractures in the calibrated model is 5×10^{-7} and the storativity of the matrix 5×10^{-10} Pa^{-1}. Obviously, the calibrated model does not match the total inflow in the early times of the reinjection, although it matches quite well the later inflow and the rate of seismicity. The large errors in the early injectivity can be explained by the rather coarse grid for the matrix around the wells, from the fact that we skipped calibrating the deterministic fractures in conjunction with the permeability of the matrix, and because pressure changes at the wells are instantaneous while, it could take up to four hours for the well to reach its target uphole pressure.

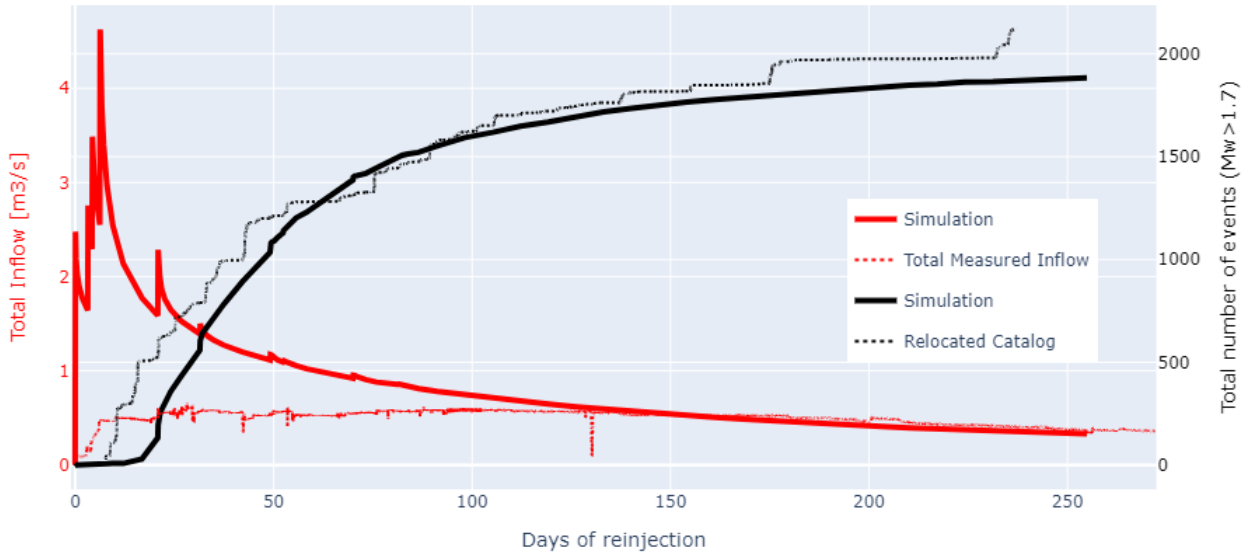

Figure 7 Simulated inflow (top) and seismicity rate (bottom) for the calibrated HFR-Sim model and its match with the observed curves.

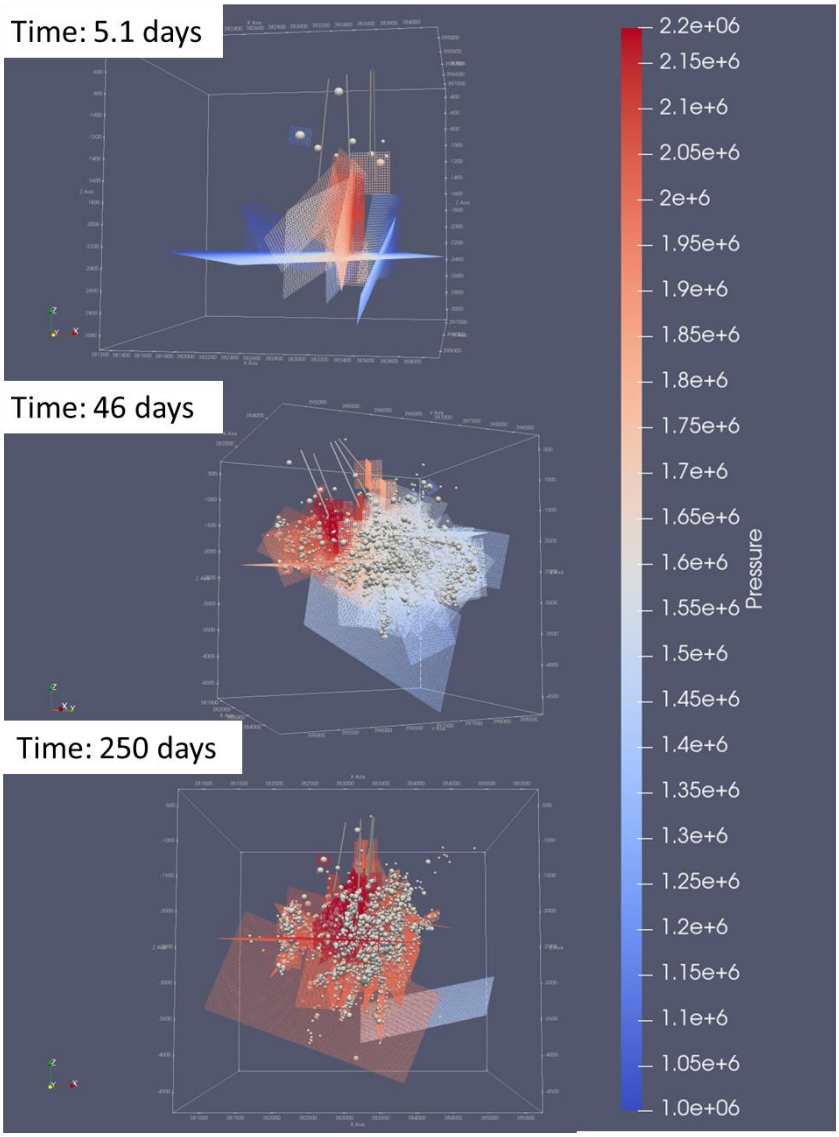

Figure 8 Snapshots of over-pressurized alignment fractures and of triggered seismicity in the calibrated HFR-Sim model.

Figure 8 shows snapshots of the evolution of overpressure in the DFN. At each snapshot, only the fracture cells with simulated overpressure above the *1 MPa* threshold are plotted. Gradually, all alignment fractures are over-pressurized. Also in the same snapshots, are plotted the seismic fractures and the triggered 'True-Positive' seeds in the calibrated model. Alignment fractures create a structural model that allows seismicity mainly where seismicity is postulated in the seismic catalog at hand.

6. CONCLUSION

A workflow is presented that utilizes hydraulic and micro-seismic data in order to calibrate high-enthalpy geothermal reservoirs. The workflow is a step towards characterizing properties of the DFN from the injection-induced micro-seismicity. The calibrated model reproduces the spatiotemporal evolution of pressure. The workflow can be part of a wider workflow since it employs a flexible DFM that combines the simplicity of continuum methods with the high fidelity of DFMs. This allows having calibrated continuum models as the starting point for further improvements to the structural model. Calibrated DFMs like the one presented here can be used for studying the positioning of future additional wells and for optimizing the water household of the field. Seismic hazard and risk predictions can be based on such a calibrated hydraulic model. Seismic and micro-seismic data can be utilized as remote pressure measurements and can reveal important deep structures.

REFERENCES

G. I. Barenblatt, Iu. P. Zheltov, and I. N. Kochina. Basic concepts in the theory of seepage of homogeneous liquids in fissured rocks [strata]. Journal of Applied Mathematics and Mechanics, 24(5):1286– 1303, January 1960.

Batir, J., Davatzes, N. C., & Asmundsson, R. (2012). Preliminary model of fracture and stress state in the Hellisheidi Geothermal Field, Hengill Volcanic System, Iceland. In Proceedings of the Thirty-Seventh Workshop on Geothermal Reservoir Engineering, Stanford.

COSEISMIQ team, (2020) "Coupled geo-mechanical and reservoir modeling framework implemented within RISC, ready for real-time application and adopted to Icelandic conditions. Integration of the methods developed in the WP2, WP3 and WP4 in a single tool (the RISC tool).", Deliverable 3 of the project, www.coseismiq.ethz.ch/en/home/

Deb, R. & Jenny, P., 2017a. Finite volume-based modeling of flow-induced shear failure along fracture manifolds, Int. J. Numer. Anal. Methods Geomech., 41 18, 1922–1942.

Deb, R. & Jenny, P., 2017b. Modeling of shear failure in fractured reservoirs with a porous matrix, Comput. Geosci., 21(5–6), 1119–1134.

Deb, R. & Jenny, P., 2017c. Finite volume-based modeling of flow-induced shear failure along fracture manifolds, Int. J. Numer. Anal. Methods Geomech., 41(18), 1922–1942

DiPippo Ronald, 2016, Geothermal Power Generation – Developments and Innovation, Book, ISBN 978-0-08-100337-4, https://doi.org/10.1016/C2014-0-03384-9

Edwards B., Douglas J.. Selecting ground-motion models developed for induced seismicity in geothermal areas, Geophys. J. Int., 2013, vol. 195 (pg. 1314-1322)

Golder Associates Inc.. (2020). Utah FORGE: Discrete Fracture Network (DFN) Data [data set]. Retrieved from https://dx.doi.org/10.15121/1776595.

Gunnarsson, G., Arnaldsson, A., & Oddsdóttir, A. L. (2011). Model simulations of the Hengill area, Southwestern Iceland. Transport in porous media, 90(1), 3-22.

Gunnarsson, G. (2013). Temperature Dependent Injectivity and Induced Seismicity–Managing Reinjection in the Hellisheiði Field, SW-Iceland. GRC Transactions, 37, 1020-1025.

Gunnar GUNNARSSON, Anette K. MORTENSEN, (2016) Dealing with Intense Production Density: Challenges in Understanding and Operating the Hellisheiði Geothermal Field, SW-Iceland. In Proceedings of the Forty-First Workshop on Geothermal Reservoir Engineering, Stanford.

Juncu, D., Árnadóttir, T., Geirsson, H., Guðmundsson, G., Lund, B., Gunnarsson, G., Hooper, A., Hreinsdóttir, S., & Michalczewska, K. (2020). Injection-induced surface deformation and seismicity at the Hellisheidi geothermal field, Iceland. Journal of Volcanology and Geothermal Research, 391, 106337. https://doi.org/10.1016/j.jvolgeores.2018.03.019

Karvounis, D.C., 2013. Simulations of enhanced geothermal systems with an adaptive hierarchical fracture representation, Doctoral thesis, Department of Mechanical and Process Engineering, Institute of Fluid Dynamics, ETH.

Karvounis D. and Jenny P. (2016), Adaptive Hierarchical Fracture Model for Enhanced Geothermal Systems, Multiscale Modeling & Simulation 2016 14:1, 207-231

Karvounis D., Wiemer S., A discrete fracture hybrid model for forecasting diffusion-induced seismicity and power generation in enhanced geothermal systems, Geophysical Journal International, Volume 230, Issue 1, July 2022, Pages 84–113, https://doi.org/10.1093/gji/ggac056

Kristjánsdóttir,B. (2018) Seismic catalog, ISOR.

Li, K. L., Abril, C., Gudmundsson, O., & Gudmundsson, G. B. (2019). Seismicity of the Hengill area, SW Iceland: Details revealed by catalog relocation and collapsing. *Journal of Volcanology and Geothermal Research*, *376*, 15-26. https://doi.org/10.1016/j.jvolgeores.2019.03.008

Mahzari, P., Stanton-Yonge, A., Sanchez-Roa, C., Saldi, G., Mitchell, T., Oelkers, E. H., Hjorleifsdottir, V., Snaebjornsdottir, S. O., Ratouis, T., Striolo, A., & Jones, A. P. (2021). Characterizing fluid flow paths in the Hellisheidi geothermal field using detailed fault mapping and stress-dependent permeability. *Geothermics*, *94*, 102127. https://doi.org/10.1016/j.geothermics.2021.102127

Moinfar, Ali , Narr, Wayne , Hui, Mun-Hong , Mallison, Bradley , and Seong H. Lee. "Comparison of Discrete-Fracture and Dual-Permeability Models for Multiphase Flow in Naturally Fractured Reservoirs." Paper presented at the SPE Reservoir Simulation Symposium, The Woodlands, Texas, USA, February 2011. doi: https://doi.org/10.2118/142295-MS

Paulillo, Andrea & Striolo, Aberto & Lettieri, Paola. (2019). The environmental impacts and the carbon intensity of geothermal energy: A case study on the Hellisheiði plant. Environment international. 133. 105226. 10.1016/j.envint.2019.105226.

Poux, Bastien & Gunnarsdóttir, Sveinborg & O´Brien, Jeremy. (2019). 3-D Modeling of the Hellisheiði Geothermal Field, Iceland, using Leapfrog. GRC Transactions, Vol. 42, 2018

Ratouis, T.M., Snæbjörnsdóttir, S.Ó., Gunnarsson, G.I., Gunnarsson, I., Kristjansson, B., Aradóttir, E.S., Bæjarhálsi, & Ratouis, T.M. (2019). Modelling the Complex Structural Features Controlling Fluid Flow at the CarbFix 2 Reinjection Site , Hellisheiði Geothermal Power Plant , SW-Iceland. In Proceedings of the Forty-Fourth Workshop on Geothermal Reservoir Engineering, Stanford.

Sigfússon, B., Arnarson, M. Þ., Snæbjörnsdóttir, S. Ó., Karlsdóttir, M. R., Aradóttir, E. S., & Gunnarsson, I. (2018). Reducing emissions of carbon dioxide and hydrogen sulphide at Hellisheidi power plant in 2014-2017 and the role of CarbFix in achieving the 2040 Iceland climate goals. *Energy Procedia*, *146*, 135-145. https://doi.org/10.1016/j.egypro.2018.07.018

Sveinbjornsson, Bjorn & Thorhallsson, Sverrir. (2013). Drilling performance and productivity of geothermal wells - Case history from Hengill Geothermal Area in Iceland. ARMA 2013 47th U.S. Rock Mechanics/Geomechanics Symposium

Zareidarmiyan, A., Parisio, F., Makhnenko, R. Y., Salarirad, H., & Vilarrasa, V. (2021). How equivalent are equivalent porous media? Geophysical Research Letters, 48, e2020GL089163. https://doi.org/10.1029/2020GL089163

ACKNOWLEDGEMENTS

Data was provided by ISÓR, Reykjavík Energy, and the Icelandic Meteorological Office (IMO). Special thanks to Reykjavik Energy for providing the large-scale TOUGH2 model. COSEISMIQ project funded this research. COSEISMIQ is subsidised through Cofund GEOTHERMICA with the European Commission and by various National Funding Agencies including the Swiss Federal Office of Energy. COSEISMIQ is supported by the European Union's HORIZON 2020 program for research, technological development, and demonstration under grant agreement No 731117.